CERN.TH/99–224

ACT-7-99

CTP-TAMU-30-99

OUTP–99–35P

astro-ph/9907340

# Astrophysical Probes of the Constancy of the Velocity of Light

**John Ellis**

Theory Division, CERN, CH-1211 Geneva 23, Switzerland

**K. Farakos**

Department of Physics, National Technical University of Athens, Zografou Campus, GR 157 80 Athens, Greece

**N.E. Mavromatos**

Department of Physics, University of Oxford, 1 Keble Road, Oxford OX1 3NP, U.K., and Theory Division, CERN, CH-1211 Geneva 23, Switzerland

**V.A. Mitsou**

Experimental Physics Division, CERN, CH-1211 Geneva 23, Switzerland. and Department of Physics, University of Athens, Panepistimioupolis Zografou GR 157 71 Athens, Greece

**D.V. Nanopoulos**

Department of Physics, Texas A & M University, College Station, TX 77843-4242, USA, Astroparticle Physics Group, Houston Advanced Research Center (HARC), Mitchell Campus, Woodlands, TX 77381, USA, and Academy of Athens, Chair of Theoretical Physics, Division of Natural Sciences, 28 Panepistimiou Avenue, GR 10679 Athens, Greece

**Abstract**

We discuss possible tests of the constancy of the velocity of light using distant astrophysical sources such as gamma-ray bursters (GRBs), Active Galactic Nuclei (AGNs) and pulsars. This speculative quest may be motivated by some models of quantum fluctuations in the space-time background, and we discuss explicitly how an energy-dependent variation in photon velocity $\delta c/c \sim -E/M$ arises in one particular quantum-gravitational model. We then discuss how data on GRBs may be used to set limits on variations in the velocity of light, which we illustrate using BATSE and OSSE observations of the GRBs that have recently been identified optically and for which precise redshifts are available. We show how a regression analysis can be performed to look for an energy-dependent effect that should correlate with redshift. The present data yield a limit $M \gtrsim 10^{15}$ GeV for the quantum gravity scale. We discuss the prospects for improving this analysis using future data, and how one might hope to distinguish any positive signal from astrophysical effects associated with the sources.

## 1. Introduction

The constancy of the velocity of light is one of the most basic tenets of modern physics. It rests on a firm experimental basis and is embedded in Lorentz invariance and the Special and General Theories of Relativity, as well as Quantum Field Theory. It may therefore seem absurd to question the constancy of the velocity of light, and unnecessary to propose testing it. Nevertheless, we think one should keep such a basic precept under review, and seize any new experimental opportunity to test it more severely than before, particularly if there are any theoretical speculations that might lead one to question it.

We believe (Amelino-Camelia *et al.* 1998) that just such an opportunity to test the constancy of the velocity of light is provided by transient astrophysical sources of $\gamma$ rays, such as gamma-ray bursters (GRBs) (Piran 1999, Rees 1997), active galactic nuclei (AGNs) and pulsars. We also believe (Ellis, Mavromatos & Nanopoulos 1999) that modern approaches to the quantization of gravity provide some motivation for exploring the opportunities provided by these astrophysical sources. The primary purpose of this paper is to review these opportunities and to make some tentative steps towards exploiting them, by proposing and pioneering some techniques for analyzing the data. This is particularly timely because we expect large amounts of useful observations of GRBs and AGNs to become available in the near future.

The primary tool for measuring small variations $\delta c$ in the velocity of light $c$ is the variation in arrival time (Amelino-Camelia *et al.* 1997, Amelino-Camelia *et al.* 1998) $\delta t \simeq -(L/c)\ (\delta c/c)$ observed for a photon travelling a distance $L$. This clearly places a premium on observing sources whose emissions exhibit structure on short time scales $\Delta t \lesssim \delta t$ located at large distances. Some typical numbers for some astrophysical sources are shown in Table 1. The relevant photon property that could be correlated with velocity variations $\delta c$ is its frequency $\nu$, or equivalently its energy $E$, for which characteristic values

are also listed in Table 1. As we discuss in more detail later, any such effect could be expected to increase with $E$, and the simplest possibility, for which there is some theoretical support, is that $\delta c \propto E/M$, where $M$ is some high energy scale. In this case, the relevant figure of merit for observational tests is the combination

$$\frac{L \cdot E}{c \cdot \delta t} \tag{1}$$

which measures directly the experimental sensitivity to such a high energy scale M. This sensitivity is also listed in Table 1, where we see that our favoured astrophysical sources are potentially sensitive to $M$ approaching $M_P \simeq 10^{19}$ GeV, the mass scale at which gravity becomes strong. Therefore, these astrophysical sources may begin to challenge any theory of quantum gravity that predicts such a linear dependence of $\delta c$ on $E$. Alternatively, it could be that $\delta c/c \simeq (E/\tilde{M})^2$, in which case the appropriate figure of merit is $E\sqrt{L/c\delta t}$, which is also listed in Table 1. In this case, we see that astrophysical observations may be sensitive to $\tilde{M} \sim 10^{11}$ TeV.

Having established the existence of an observational opportunity, we now try to give some flavour of the theoretical motivation for questioning the constancy of the velocity of light, in the context of a quantum theory of gravity. A preliminary remark is that any attempt to quantize gravity canonically must involve a Lorentz-non-invariant separation of degrees of freedom and the choice of a preferred reference frame. There is a natural local rest-frame in our approximately Friedman-Robertson-Walker Universe, namely the comoving frame identified approximately by the cosmic microwave background radiation. This provides a natural frame in which to consider topological fluctuations in the space-time background, as might arise from microscopic black holes or other non-perturbative phenomena in quantum gravity – the so-called space-time foam (Wheeler 1963, Hawking, Page & Pope 1980, Hawking 1982, Ellis *et al.* 1984, Ellis, Mavromatos & Nanopoulos 1992, Garay 1998, Ellis, Mavromatos & Nanopoulos 1999).

**Table 1: Observational Sensitivities and Limits on $M, \tilde{M}$**

| Source | Distance | $E$ | $\Delta t$ | Sensitivity to $M$ | Sensitivity to $\tilde{M}$ |
|---|---|---|---|---|---|
| GRB 920229 [a] | 3000 Mpc (?) | 200 keV | $10^{-2}$ s | $0.6 \times 10^{16}$ GeV (?) | $10^6$ GeV (?) |
| GRB 980425 [a] | 40 Mpc | 1.8 MeV | $10^{-3}$ s (?) | $0.7 \times 10^{16}$ GeV (?) | $3.6 \times 10^6$ GeV (?) |
| GRB 920925c [a] | 40 Mpc (?) | 200 TeV (?) | 200 s | $0.4 \times 10^{19}$ GeV (?) | $8.9 \times 10^{11}$ GeV (?) |
| Mrk 421 [b] | 100 Mpc | 2 TeV | 280 s | $> 7 \times 10^{16}$ GeV | $> 1.2 \times 10^{10}$ GeV |
| Crab pulsar [c] | 2.2 kpc | 2 GeV | 0.35 ms | $> 1.3 \times 10^{15}$ GeV | $> 5 \times 10^7$ GeV |
| GRB 990123 | 5000 Mpc | 4 MeV | 1 s (?) | $2 \times 10^{15}$ GeV (?) | $2.8 \times 10^6$ GeV (?) |

[a] Amelino-Camelia *et al.* 1998, *see also* Schaefer 1998

[b] Biller *et al.* 1998

[c] Kaaret 1999

Table 1: *The linear (quadratic) mass-scale parameters $M, \tilde{M}$ are defined by $\delta c/c = E/M, (E/\tilde{M})^2$, respectively. The question marks in the Table indicate uncertain observational inputs. Hard limits are indicated by inequality signs.*

Initially in the context of a string approach (Amelino-Camelia *et al.* 1997), it has been argued that foamy effects might lead the quantum-gravitational vacuum to behave as a non-trivial medium, much like a plasma or other environment with non-trivial optical properties. Another possible example of such behaviour has been proposed within a canonical approach to quantum gravity (Gambini & Pullin 1999, and it has also been observed that quantum fluctuations in the light-cone are to be expected (Yu & Ford 1999). The basic intuition behind such suggestions is that quantum-gravitational fluctuations in the vacuum must in general be modified by the passage of an energetic particle, and that this recoil will be reflected in back-reaction effects on the propagating particle itself.

Three possible optical effects of quantum gravity have been identified. One is a simple energy-dependent reduction in photon velocity, namely a frequency-dependent refractive index (Amelino-Camelia *et al.* 1997, Amelino-Camelia *et al.* 1998). The second is a possible difference between the velocities of photons of different helicities, namely birefringence (Gambini & Pullin 1999). An opportunity for an experimental test of such a phenomenon has been provided recently by the observations of polarized radiation from GRB 990510 (Covino *et al.* 1999, Wijers *et al.* 1999). The third is a possible energy-dependent diffusive spread in the velocities of different photons of the same energy (Ellis, Mavromatos & Nanopoulos 1999, Ford 1995, Yu & Ford 1999). In each case, the relevant figure of merit would be (1) if the effect is linear in energy.

Most of the rest of this paper constitutes a phenomenological analysis of issues involved in the search for any such effect, and in disentangling it from phenomena at the source, which we illustrate by a prototype analysis of the available data on GRBs with established redshifts, with the results listed in Table 2 and 3. Such an analysis has been made possible by the data from the BeppoSAX satellite (Boella *et al.* 1997), which made it possible to observe afterglows from identified GRBs, and measure their redshifts for the first time.

However, we first provide in Section 2 a simple analysis of the refractive index induced by one particular recoil model for the quantum-gravitational medium, which provides some physical flesh for the conceptual skeleton outlined in this Introduction. In Sections 3 and 4 we discuss the propagation of a pulse of electromagnetic radiation produced by an ultra-relativistic source, as in a GRB explosion. Then, in Section 5 we discuss how one may fit structures observed in the available GRB data, and analyze their energy-dependence to look for medium effects. As we shall see, a key issue is to distinguish any such medium effects from effects at the source. The former should increase when one considers GRBs at larger distance $L$ or redshift $z$. We perform in Section 5 a prototype regression analysis of

the data from the handful of GRBs whose redshifts are currently known. Unsurprisingly, the present data do not exhibit any significant correlation with $z$, but the method could usefully be extended to the hundreds of GRBs whose redshifts are expected to be measured in coming years. What if such a future analysis should yield a significant effect? It should certainly not be believed without very critical review, and some of the issues in the astrophysical modelling of GRBs and the correlation of data from other sources such as AGNs are reviewed in the concluding Section 6.

## 2. Quantum-Gravitational Recoil Effects on the Propagation of Electromagnetic Waves

Our intuitive picture is that the quantum-gravitational vacuum contains quantum fluctuations with typical sizes $\sim l_P \sim 10^{-33}$ cm and time-scales $\sim t_P \sim 10^{-43}$ s. We then hypothesize that particles propagating through the vacuum interact with these fluctuations, inducing non-trivial recoil and associated vacuum-polarization effects. As a specific example, we have used the theoretical model of a recoiling $D$ particle in the quantum-gravitational foam. Its recoil due to scattering by a photon has been argued (Ellis, Mavromatos & Nanopoulos 1998) to lead to a non-zero gravitational field with a metric of the form (Ellis *et al.* 1998):

$$G_{ij} = \delta_{ij},\ G_{00} = -1,\ G_{0i} = \epsilon^2(Y_i + \overline{U}_i t)\Theta_\epsilon(t) \tag{2}$$

where $0(i)$ denote time (space) components. Here, $\overline{U}_i$ is the recoil velocity of the $D$ particle, which is located at $Y_i$, and $\epsilon$ is a small parameter. The metric (2) implies that $D$-brane recoil induces the following perturbation $h_{\mu\nu}$ about flat space-time:

$$h_{0i} = \epsilon^2 \overline{U}_i t \Theta_\epsilon(t) \tag{3}$$

where we have only indicated the only non-zero components of $h_{\mu\nu}$.

We may identify $\epsilon^{-2} \sim t$ at large times, so that the asymptotic form of the gravitational perturbation takes the form:

$$h_{0i} \sim \overline{U}_i \tag{4}$$

We note that this form corresponds to a breakdown of Lorentz invariance induced by the propagation of the photon: for symmetry reasons, any perturbation induced by other models might be expected to take a similar form. We suppose that the light travels a distance $L$ in time $t \sim \epsilon^{-2}$ in the presence of a metric fluctuation $h_{0i}$ given by (4). The effects of such a field in Maxwell's equations have been considered previously (Ellis, Mavromatos & Nanopoulos 1999): here we present an elementary analysis, which does not require any string or quantum field theory formalism. In fact, is interesting to note that the interpretation of Maxwell's equations in the presence of a background gravitational field, with a non-diagonal component $g_{0i}$ was proposed as an exercise for the reader by Landau and Lifshitz (Landau & Lifshitz 1975), where a *formal* analogy with the propagation in a medium has been noted.

We parametrize the background metric in the form:

$$G_{00} \equiv -h, \qquad \mathcal{G}_i = -\frac{G_{0i}}{G_{00}}, \qquad i = 1, 2, 3 \tag{5}$$

Maxwell's equations in this background metric in empty space can be written as (Landau & Lifshitz 1975):

$$\begin{aligned} \nabla \cdot B = 0, \qquad & \nabla \times H = \frac{1}{c}\frac{\partial}{\partial t} D = 0, \\ \nabla \cdot D = 0, \qquad & \nabla \times E = -\frac{1}{c}\frac{\partial}{\partial t} B = 0, \end{aligned} \tag{6}$$

where

$$D = \frac{E}{\sqrt{h}} + H \times \mathcal{G}, \qquad B = \frac{H}{\sqrt{h}} + \mathcal{G} \times E \tag{7}$$

Thus, there is a direct analogy with Maxwell's equations in a medium with $1/\sqrt{h}$ playing the rôle of the electric and magnetic permeability. In our case (Ellis, Mavromatos &

Nanopoulos 1998), $h = 1$, so one has the same permeability as the classical vacuum. In the case of the constant metric perturbation (4), after some elementary vector algebra and, appropriate use of the modified Maxwell's equations, the equations (6) read:

$$\begin{aligned}
&\nabla \cdot E + \overline{U} \cdot \frac{1}{c}\frac{\partial}{\partial t} E = 0 \\
&\nabla \times B - \left(1 - \overline{U}^2\right) \frac{1}{c}\frac{\partial}{\partial t} E + \overline{U} \times \frac{1}{c}\frac{\partial}{\partial t} B + \left(\overline{U} \cdot \nabla\right) E = 0 \\
&\nabla \cdot B = 0 \\
&\nabla \times E + \frac{1}{c}\frac{\partial}{\partial t} B = 0
\end{aligned} \tag{8}$$

Dropping non-leading terms of order $\overline{U}^2$ from these equations, one obtains after some straightforward algebra the following modified wave equations for $E$ and $B$:

$$\begin{aligned}
&\frac{1}{c^2}\frac{\partial^2}{\partial^2 t} B - \nabla^2 B - 2\left(\overline{U}.\nabla\right)\frac{1}{c}\frac{\partial}{\partial t} B = 0 \\
&\frac{1}{c^2}\frac{\partial^2}{\partial^2 t} E - \nabla^2 E - 2\left(\overline{U}.\nabla\right)\frac{1}{c}\frac{\partial}{\partial t} E = 0
\end{aligned} \tag{9}$$

If we consider one-dimensional motion along the $x$ direction, we see that these equations admit wave solutions of the form

$$E_x = E_z = 0,\ E_y(x,t) = E_0 e^{ikx-\omega t},\ \ B_x = B_y = 0,\ B_z(x,t) = B_0 e^{ikx-\omega t}, \tag{10}$$

with the modified dispersion relation:

$$k^2 - \omega^2 - 2\overline{U} k\omega = 0 \tag{11}$$

Since the sign of $\overline{U}$ is that of the momentum vector $k$ along the $x$ direction, the dispersion relation (11) corresponds to *subluminal* propagation with a refractive index:

$$c(E) = c\left(1 - \overline{U}\right) + \mathcal{O}\left(\overline{U}^2\right) \tag{12}$$

where we estimate that

$$\overline{U} = \mathcal{O}\left(\frac{E}{M_D c^2}\right) \tag{13}$$

with $M_D$ the $D$-particle mass scale. This is in turn given by $M_D = g_s^{-1} M_s$ in a string model, where $g_s$ is the string coupling and $M_s$ is the string scale (Ellis, Mavromatos & Nanopoulos 1999). The relation (13) between $\overline{U}$ and the photon energy has been shown (Lizzi & Mavromatos 1997, Mavromatos & Szabo 1998, Ellis, Mavromatos & Nanopoulos 1998) to follow from a rigorous world-sheet analysis of modular divergences in string theory, but the details need not concern us here. It merely expresses elementary energy-momentum conservation.

The refractive index effect (13) is a mean-field effect, which implies a delay in the arrival times of photons, relative to that of an idealized low-energy photon for which quantum-gravity effects can be ignored, of order:

$$\Delta t \sim \frac{L}{c} |\overline{U}| = \mathcal{O}\left(\frac{EL}{M_D c^3}\right) \tag{14}$$

We have discussed in some detail (Ellis, Mavromatos & Nanopoulos 1999) the quantum fluctuations about the mean-field solution (14), which would correspond in field theory to quantum fluctuations in the light cone, and could be induced by higher-genus effects in a string approach. Such effects would result in stochastic fluctuations in the velocity of light which are of order

$$\delta c \sim 8 g_s E / M_D c^2, \tag{15}$$

where $g_s$ is the string coupling, which varies between $\mathcal{O}(1)$ and $\ll 1$ in different string models. Such an effect would motivate the following parametrization of any possible stochastic spread in photon arrival times:

$$(\delta \Delta t) = \frac{LE}{c\Lambda} \tag{16}$$

where the string approach suggests that $\Lambda \sim M_D c^2 / 8 g_s$. We emphasize that, in contrast to the variation (13) in the refractive index - which refers to photons of different energy - the fluctuation (16) characterizes the statistical spread in the velocities of photons *of the same*

*energy*. Note that the stochastic effect (16) is suppressed, as compared to the refractive index mean field effect (13), by an extra power of $g_s$.

## 3. Propagation of a Pulse of Photons through the Space-Time Foam

GRBs typically emit photons in pulses containing photons with a combination of different wavelengths, whose sources are believed to be ultrarelativistic shocks with Lorentz factors $\gamma = \mathcal{O}(100)$ (Piran 1999, Rees 1997). We do not enter here into the details of the astrophysical modelling of such sources. This is unnecessary for our present exploratory study, though it may be essential for future more detailed probes of the constancy of the velocity of light. Instead, here we study a simple generalization of the previous discussion of monochromatic wave propagation, considering a wave packet of photons emitted with a Gaussian distribution in the light-cone variable $x - ct$. Since the distance over which the ultrarelativistic source moves during the emission is negligible compared with the distance between the source and the observer, we may represent the source equally well with a Gaussian distribution in $x$ at the time $t = 0$. This is adequate to see how such a pulse would be modified at the observation point at a subsequent time $t$, because of the propagation through the space-time foam, as a result of the refractive index effect (11), (12). The phenomenon is similar to the motion of a wave packet in a conventional dispersive medium, as discussed extensively in the standard literature.

The Gaussian wavepacket may be expressed at $t = 0$ as the real part of

$$f(x) = Ae^{-x^2/(\Delta x_0)^2} e^{ik_0 x} \tag{17}$$

with a modulation envelope that is symmetrical about the origin, where it has amplitude $A$. The quantity $\Delta x_0$ in (17) denotes the root mean square of the spatial spread of the energy distribution in the packet, which is proportional to $|f(x)|^2$, as is well known. If we assume

a generic dispersion relation $\omega = \omega(k)$, a standard analysis using Fourier transforms shows that at time $t$ the Gaussian wavepacket will have the form:

$$|f(x,t)|^2 = \frac{A^2}{(1+\frac{\alpha^2 t^2}{(\Delta x_0)^4})^{1/2}} e^{-\frac{(x-c_g t)^2}{\left(2(\Delta x_0)^2[1+\frac{\alpha^2 t^2}{(\Delta x_0)^4}]\right)}} \tag{18}$$

where $\alpha \equiv \frac{1}{2}\,(d^2\omega/d^2k)$, and $c_g \equiv d\omega/dk$ is the group velocity. This is the velocity with which the peak of the distribution moves in time.

We see immediately in (18) that the quadratic term $\alpha$ in the dispersion relation does not affect the motion of the peak, but only the spread of the Gaussian wave packet:

$$|\Delta x| = \Delta x_0 \left(1 + \frac{\alpha^2 t^2}{(\Delta x_0)^4}\right)^{1/2} \tag{19}$$

which thus increases with time. The quadratic term $\alpha$ also affects the amplitude of the wave packet: the latter decreases together with the increase in the spread (19), in such a way that the integral of $|f(x,t)|^2$ is constant.

In the case of the quantum-gravitational foam scenario (Ellis, Mavromatos & Nanopoulos 1999, Amelino-Camelia *et al.* 1997), the dispersion relation assumes the following form for positive momentum $k$, in units where $c = \hbar = 1$:

$$\begin{aligned} k &= \omega\left(1 + \frac{\omega}{M_D}\right) \text{ or } \omega = k\left(1 - \frac{k}{M_D} + \ldots\right) \\ c_g &== \left(1 - \overline{U}\right) = 1 - \mathcal{O}\left(\omega/M_D\right), \\ \alpha &= -\frac{1}{M_D} + \ldots \end{aligned} \tag{20}$$

where we denote by $\ldots$ denotes the higher-order (e.g., quadratic) terms in $1/M_D$, which are subleading in this case. Thus the spread of the wave packet due to the non-trivial refractive index effect described in the previous section is:

$$|\Delta x| = \Delta x_0 \left(1 + \frac{t^2}{M_D^2 (\Delta x_0)^4}\right)^{1/2} \tag{21}$$

We note that the spread due to the refractive index $\delta c/c \propto \omega$ is independent of the energy of the photon to leading order in $1/M_D$. We also note, therefore, that this effect is distinct from the stochastic propagation effect, which gives rise to a spread (16) in the wave-packet that depends on the photon energy $\omega$. For astrophysical sources at cosmological distances with redshifts $z \simeq 1$, and with an initial $\Delta x_0$ of a few km, one finds that the correction (21) is negligible if the quantum-gravity scale $M_D$ is of the order of $10^{19}$ GeV, namely of order $10^{-30}\Delta x_0$. The correction would become of order $\Delta x_0$ only if the latter is of order $10^{-3}$ m. Even if one allows $M_D$ to be as low as the sensitivities shown in Table 1, this broadening effect is still negligible for all the sources there, being at most of order $10^{-22}\Delta x_0$. Therefore, in this particular model, the only broadening effect that needs to be considered is the stochastic quantum-gravitational effect on the refractive index that was introduced at the end of the previous section.

In the case of a quantum-gravitational foam scenario with a quadratic refractive index: $\delta c/c \sim E^2$, the dispersion relation assumes the following form:

$$\begin{aligned} k &= \omega\left(1+\frac{\omega}{\tilde{M}}\right) \text{ or } \omega = k\left(1-\left(\frac{k}{\tilde{M}}\right)^2+\ldots\right) \\ c_g &== \left(1-\overline{U}\right) = 1-\mathcal{O}\left(\omega^2/\tilde{M}^2\right), \\ \alpha &= -3\frac{\omega}{\tilde{M}}+\ldots \end{aligned} \tag{22}$$

where ... again denote subleading terms. In this case, the spread of the wave packet due to the non-trivial refractive index effect described above is:

$$|\Delta x| = \Delta x_0\left(1+\frac{9\omega^2 t^2}{\tilde{M}^4(\Delta x_0)^4}\right)^{1/2} \tag{23}$$

Once again, if one takes into account the sensitivities shown in Table 1, the maximum spreading of the pulse is negligible for $\Delta x_0 \sim 10^{-3}$ m, namely at most $\sim 10^{-33}\Delta x_0$. Once again, one would need only to consider the possible stochastic quantum-gravitational effect on the refractive index. However, since a quadratic dependence is not favoured theoretically,

we do not pursue it further in the rest of this paper.

## 4. Cosmological Expansion and Light Propagation

We now discuss the implications of the cosmological expansion for the searches for a quantum-gravity induced refractive index (14) and a stochastic effect (16). We work within the general context of Friedman-Robertson-Walker (FRW) metrics, as appropriate for standard homogeneous and isotropic cosmology (Weinberg 1972). We denote by $R$ the FRW scale factor, adding a subscript 0 to denote the value at the present era, $H_0$ is the present Hubble expansion parameter, and the deceleration parameter $q_0$ is defined in terms of the curvature $k$ of the FRW metric by $k = (2q_0 - 1)(H_0^2 R_0^2/c^2)$, i.e., $\Omega_0 = 2q_0$.

Motivated by inflation and the cosmic microwave background data, we assume a Universe with a critical density: $\Omega_0 = 1$, $k = 0$ and $q_0 = 1/2$. We also assume that the Universe is matter-dominated during all the epoch of interest. Then the scale factor $R(t)$ of the Universe expands as:

$$\frac{R(t)}{R_0} = \left(\frac{3H_0}{2}\right)^{2/3} t^{2/3} \tag{24}$$

and the current age of the Universe is

$$t_0 = \frac{2}{3H_0} \tag{25}$$

Clearly no time delay can be larger than this. The relation between redshift and scale factor is

$$R(t)/R_0 = 1/(1+z) \tag{26}$$

Substituting (26) into (24), we find the age of the Universe at any given redshift:

$$t = (\frac{2}{3H_0})\frac{1}{(1+z)^{3/2}} = \frac{t_0}{(1+z)^{3/2}} \tag{27}$$

Hence, a photon (or other particle) emitted by an object at redshift $z$ has travelled for a time

$$t_0 - t = \frac{2}{3H_0}\left(1 - \frac{1}{(1+z)^{3/2}}\right) \tag{28}$$

The corresponding differential relation between time and redshift is

$$dt = -\frac{1}{H_0}\frac{1}{(1+z)^{5/2}}dz \tag{29}$$

This means that during the corresponding infinitesimal time (redshift) interval, a particle with velocity $u$ travels a distance

$$u\,dt = -\frac{1}{H_0}\frac{u}{(1+z)^{5/2}}dz. \tag{30}$$

Therefore, the total distance $L$ travelled by such a particle since emission at redshift $z$ is

$$L = \int_t^{t_0} u dt = \frac{1}{H_0}\int_0^z \frac{u(z)}{(1+z)^{5/2}}dz \tag{31}$$

hence, the difference in distances covered by two particles with velocities differing by $\Delta u$ is:

$$\Delta L = \frac{1}{H_0}\int_0^z \frac{dz}{(1+z)^{5/2}}(\Delta u) \tag{32}$$

where we allow $\Delta u$ to depend on $z$.

In the context of our quantum-gravity-induced refractive-index phenomenon (13), we are confronted with just such a situation. Consider in that context two photons travelling with velocities very close to $c$, whose present-day energies are $E_1$ and $E_2$. At earlier epochs, their energies would have been blueshifted by a common factor $1+z$. Defining $\Delta E_0 \equiv E_1 - E_2$, we infer from (13) that $\Delta u = (\Delta E_0 \cdot (1+z))/M$. Inserting this into (32), we find an induced difference in the arrival time of the two photons given by

$$\Delta t = \frac{\Delta L}{c} \simeq \frac{2}{H_0}\left[1 - \frac{1}{(1+z)^{1/2}}\right]\frac{\Delta E_0}{M}. \tag{33}$$

The expression (33) describes the corrections to the refractive index effect (14) due to the cosmological expansion. For small $z << 1$, the general expression (33) yields

$\Delta t \simeq (z \cdot \Delta E_0)/(H_0 \cdot M)$, which agrees with the simple expectation $\Delta t \simeq (r \cdot \Delta E_0)/(c \cdot M)$ for a nearby source at distance $r = c(t_0 - t) \simeq z/H_0 + \ldots$. There would be similar cosmological corrections to the stochastic effect (16), also given by an expression of the form (33), but with $\Delta E_0 \to E$, $M \to \Lambda$, where $E$ is a typical energy scale in a single channel.

In the next Section we present a detailed analysis of the astrophysical data for the five GRBs listed in Section 2, whose redshifts $z$ are known. We shall be looking for a correlation with the redshift, calculating a regression measure for the effect (33) and its stochastic counterpart. Specifically, we shall concentrate on looking for linear dependences of the "observed" $\Delta t/\Delta E_0$ and the spread $\Delta\sigma/E$ on $\tilde{z} \equiv 2 \cdot [1 - (1/(1+z)^{1/2}] \simeq z - (3/4)z^2 + \ldots$.

## 5. GRB Data Analysis

We present in this section a model analysis of astrophysical data on GRB pulses that allows us to place a bound on the phenomena discussed in the previous sections, motivated by possible non-trivial medium effects of quantum gravity on the propagation of photon probes. Previously, the data from individual GRBs (Amelino-Camelia *et al.* 1998, Schaefer 1998), AGNs (Biller *et al.* 1998) and pulsars (Kaaret 1999) had been considered. Here we take a further step, analyzing the data from those GRBs whose redshifts are known after identification of their optical counterparts. This enables us to perform a regression analysis to seasrch for a possible correlation with redshift (distance), as a first attempt to unravel source and medium effects. However, this analysis should only be considered as a prototype. Much more sophisticated fits to the data of individual GRBs could be attempted, but this would probably be worthwhile only when many more GRB redshifts are known. We anticipate that this should be the case within a year or two. It should also be emphasized that, even if an effect correlated with redshift were to be detected, it would still be necessary to confirm that it was a medium effect rather than an evolutionary effect in the GRB

sources. This would surely require detailed astrophysical sources and/or a confirmation of a similar effect in emissions from a different population of distant astrophysical sources, such as AGNs. However, these topics lie beyond the scope of the present article.

In our searches for the effects described in Sections 2 and 3, we look for short-duration structures in the time profiles of those GRBs whose redshifts, and hence distances, are known with some precision. We then make appropriate fits of the astrophysical data in various energy channels, seeking to constrain differences in the timings and widths of peaks for different energy ranges. Simultaneity of the peak arrival times at different energies would place bounds on the induced refractive index (12) of photons. Independence of the widths of peaks from the channel energies would constrain stochastic fluctuations in the velocities of photons of the same energy.

The sample of GRB data discussed below have been taken from the BATSE catalogue (Paciesas *et al.* 1999) and OSSE data (OSSE 1999). We focus on the following five GRBs, whose redshifts $z$ are known:

- GRB 970508 with BATSE trigger number 6225 and redshift $z$=0.835,
- GRB 971214 with BATSE trigger number 6533 and redshift $z$=3.14,
- GRB 980329 with BATSE trigger number 6665 and redshift $z$=5.0,
- GRB 980703 with BATSE trigger number 6891 and redshift $z$=0.966,
- GRB 990123 with BATSE trigger number 7343 and redshift $z$=1.60.

We recall the energy ranges in which BATSE generally observes photons: Channel 1 in the energy range (20,50) keV, Channel 2 between (50,100) keV, Channel 3 between (100,300) keV and Channel 4 above 300 keV. We note that the energies recorded by BATSE are not

the exact photon energies, and that there is in particular some feedthrough from high-energy photons into lower-energy channels. This effect can be neglected in the pioneering analysis that we undertake here, and is sidestepped in our later comparison of BATSE and OSSE data, but may need to be taken into account in any more detailed follow-up analysis.

The data for each GRB exhibit non-trivial and non-universal structures in time. For each of the triggers studied, we have fitted one or two of the prominent peaks in each of the energy channels, with the aim of looking for or constraining their differences in time or width between different energy channels. We have explored four different functions for the fits to the different peaks: (i) a Gaussian function characterized by the peak location $t_p$ and width parameter $\sigma$, (ii) a Lorentzian function characterized by: $A/[(t-t_p)^2 + (\Gamma/2)^2]$ (iii) a 'tail' fit with fitting function

$$N(t) = c_1 * (t - t_0)^m \; exp[-(t - t_0)^2/(2 \cdot \tau^2)], \quad t > t_0 \tag{34}$$

which peaks at $t_p = \tau\sqrt{m} + t_0$, to take into account the tail that tends to appear in the data after the peak, and (iv) the phenomenological 'pulse' model of Norris et al., which has the functional form (Norris *et al.* 1996)

$$N(t) = c_1 \; \exp\left[-(\mathrm{abs}(t - t_p)/\sigma_{r,d})^\nu\right] \tag{35}$$

where $t_p$ is the time at which the photon pulse takes its maximum, $\sigma_r$ and $\sigma_d$ are the rise and decay times of the distribution, respectively, and $\nu$ gives the sharpness or smoothness of the pulse at its peak.

We compare in Fig. 1 the four fits to the data for GRB 970508 in Channels 1 and 3. As seen in Fig. 1, the Gaussian and Lorentzian fits are of lower quality than the 'tail' and 'pulse' fits, so we concentrate on the latter for the remaining GRBs. Figs. 2 to 5 show the 'tail' and 'pulse' fits for the remaining GRBs that we study: 971214, 980329, 980703 and 990123, respectively. We compile in Table 2 the values of the 'tail' and 'pulse' fit parameters

that we find for all the GRBs. Specifically, we list for both the 'tail' and 'pulse' fitting functions the peak time, $t_p$, and the pulse width, $\sigma$, defined as half of the width of the pulse at $e^{-1/2} \simeq 60\%$ of its maximum value. When applied to the 'tail' distribution (34), this definition yields

$$\sigma = \alpha\tau\sqrt{m}, \tag{36}$$

where $\tau$ and $m$ are defined in (34), and $\alpha > 0$ is the solution of the equation

$$\ln(1+\alpha) - \frac{1}{2}(1+\alpha)^2 + \frac{1}{2}(1+m^{-1}) = 0, \tag{37}$$

whilst for the 'pulse' distribution this definition yields $\sigma = (\sigma_r + \sigma_d)/2$.

The values recorded in Table 2 may be of more general interest to those modelling GRBs. However, our main interest here is to compare the values of these parameters in the different channels, and use their differences to constrain energy-dependent differences and stochastic fluctuations in photon velocities. As seen in Table 2, we find that the different fitting functions yield constraints on the propagation parameters that are comparable within the statistical errors: we use the differences between them as gauges of the systematic errors.

The only candidate that we see for a systematic trend in the data is a tendency for pulses in the higher-energy channels to be narrower than in the lower-energy channels. This effect is seen clearly in Fig. 1 for the case of GRB 970508. However, this narrowing is the opposite of what we would suggest theoretically, which would be a slowing and broadening of the peak at higher energies.

We also compare data from Channel 3 of the BATSE detector with the data from OSSE detector (OSSE 1999), which detects photons in a single channel with energy range $1 < E < 5 - 10$ MeV. Since the OSSE data are at higher energies, they are more sensitive to the type of energy-dependent effect of interest to us. The reason we compare the OSSE

data with Channel 3 of the BATSE data is that the latter are free of contamination by the data in lower-energy channels, removing one particular possible source of systematic error. OSSE data are available for the GRBs 980329 and 990123, which we display in Figs. 6 and 7, respectively. The results of our numerical analysis of the arrival times and widths of identified OSSE pulses are given in Table 3.

In order to investigate the possible fundamental physics significance of this or any other possible energy-dependent effect, we have compiled the data from all the GRBs we have studied as functions of the figure of merit $\tilde{z} = 1 - 1/(1+z)^{1/2}$ introduced at the end of Section 4, as seen in Fig. 8 for the locations of the peaks, and in Fig. 9 for the width parameters. In some cases, there are two BATSE points with the same redshift, reflecting the fact that we have fitted two peaks in the BATSE data for the corresponding GRB. Also plotted are the results of the OSSE analysis for the GRBs 980329 and 990123. The inner error bars in Figs. 8 and 9 are the purely statistical errors produced by the fitting routines, taking as central values those extracted from the 'pulse' fits, which we consider to be the most reliable. The outer error bars are obtained by adding in quadrature a theoretical 'systematic' error, defined by the differences between the values of the fitting parameters obtained from the 'tail' and 'pulse' fits. All the numbers used are taken from Tables 2 and 3.

No strong correlation with $z$ is apparent in either Fig. 8 or Fig. 9. We have performed a regression analysis for linear dependences of the forms

$$y(\tilde{z}) = a\tilde{z} + b \tag{38}$$

for both the time delays $y = t_p$ and the width parameters $y = \sigma$.

The extracted regression coefficients, defined by $r^2 \equiv (\sum_i (y_{\rm est} - \overline{y})^2)/(\sum_i (y - \overline{y})^2)$, where $y_{\rm est}$ is the estimated value given by (38) and $\overline{y}$ is the mean value of the experimental

data, are

$$\text{Time Delays}: \quad r^2_{t_p} = 0.11, \qquad \text{Widths}: \quad r^2_{\sigma} = 0.12, \tag{39}$$

indicating no significant correlation. As an exercise, we have repeated the regression analysis omitting individual data points, to see whether any rogue point could be concealing a significant effect: again, no significant correlation was found.

The formal results of the linear fits shown in Figs. 8 and 9 for the coefficients defined in (39) are

$$\begin{aligned} \text{Time Delays}: \qquad & a = -3.0(5), \quad b = 1.4(2), \\ \text{Widths}: \qquad & a = -1.6(6), \quad b = 0.3(2). \end{aligned} \tag{40}$$

The negative slopes of these fits are opposite in sign to those expected for the quantum-gravity refractive-index effect (33) and its stochastic fluctuations. As already discussed, the regression analysis indicates that neither of the $a$ values should be interpreted as a real effect, because of the scatters in the data sets. We determine limits on the quantum gravity scales $M$ and $\Lambda$ by identifying the magnitudes of the slopes $a$ in (40) with the coefficients of the $\tilde{z}$ terms in (33) and its equivalent for the width parameter. Using the current value for the Hubble expansion parameter, $H_0 = 100 \cdot h_0$ km/s/Mpc, where $0.6 < h_0 < 0.8$, we obtain from the the regression fits of Figs. 8 and 9 the following limits

$$M \gtrsim 10^{15} \text{ GeV}, \quad \Lambda \gtrsim 2 \times 10^{15} \text{ GeV} \tag{41}$$

on the possible quantum-gravity effects.

## 6. Conclusions and Prospects

The possibility that the velocity of light might depend on its frequency, i.e., the corresponding photon energy, is very speculative. Nevertheless, we consider the motivation

from fundamental physics and the potential significance of any possible observation to be sufficient to examine this possibility in an entirely phenomenological way. In this paper, we have attempted to extract the maximum physical information from the few GRBs whose cosmological redshifts have been measured, and for which detailed information on the time distributions of photons in different energy channels are available.

As could be expected, we have found no significant effect in the data available, either in the possible delay times of photons of higher energies, or in the possible stochastic spreads of velocities of photons with the same energy. If any effect were to be found in the distributions of photons observed, one would naturally suspect that it could be due to some source effect. Therefore, we have made a regression analysis, and found no significant correlation of either time delays of peak spreading with the measured redshifts.

We note that, because of the binning (1.024 s) of the BATSE data set used here. none of the GRBs studied in Tables 2 and 3 exhibits 'microbursts' on timescales $\sim 10^{-2}$ s (Scargle, Norris & Bonnell 1997), such as were considered previously (Amelino-Camelia *et al.* 1998): if any were to be discovered in a GRB with known redshift, the sensitivity of the subsequent analysis would be greatly increased. We expect that the redshifts of many more GRBs will become known in the near future, as alerts and follow-up observations become more effective, for example after the launch of the HETE II satellite (Ricker 1998, Hurley 1998). Also, it is clear that observations of higher-energy photons from GRBs would be very valuable, since they would provide a longer lever arm in the search for energy-dependent effects on photon propagation. Such higher-energy observations could be provided by future space experiments such as AMS (Ahlen *et al.*) and GLAST (Bloom *et al.* 1996).

Even if a correlation with redshift of delays in the arrival times of energetic photons (or of spreads in their arrival times) were to be found, one could not immediately lay the blame on fundamental physics effects on photon propagation *in vacuo*. For example, the

GRB sources might exhibit evolutionary effects that mimic a correlation with redshift. Alternatively, observational selection effects might mean that the available GRB samples at low and high redshifts would have different intrinsic properties, e.g., brightness, that could also create an artificial correlation with redshift. For example, there seems to be a general grouping of GRBs into 'short' bursts, with durations $< 2$ s, and 'longer' bursts. Because of selection effects, most of the former are believed to be at small redshifts, so the analysis could become biased if the sources of 'short' and 'long' bursts had different intrinsic time-lags between photons in different BATSE channels. In point of fact, all the GRBs whose redshifts have been determined so far are in the 'long' burst category, so this particular problem may not be important for the data set used here. However, there could be more subtle selection effects, and any more detailed phenomenological analysis of the data should proceed hand-in-hand with more sophisticated astrophysical modelling of the GRB sources.

Moreover, even if the best efforts of the astrophysical modellers failed to exclude a fundamental physics effect, any such interpretation could be considered established only if other classes of data were to confirm it. This might require analyses of other types of astrophysical sources, such as AGNs and/or pulsars. An alternative possibility would be to consider more carefully laboratory experiments that might be able to reveal possible variations in the velocity of light.

**Acknowledgements**

We thank Giovanni Amelino-Camelia, Marta Felcini, Hans Hofer, Shmuel Nussinov, Tsvi Piran, Subir Sarkar and Spiros Tzamarias for their interest and advice. The work of N.E.M. is partially supported by a P.P.A.R.C. (U.K.) Advanced Fellowship, that of V.A.M. is partially supported by the Greek State Scholarships Foundation, and that of D.V.N. is partially supported by DOE grant DE-FG03-95-ER40917.

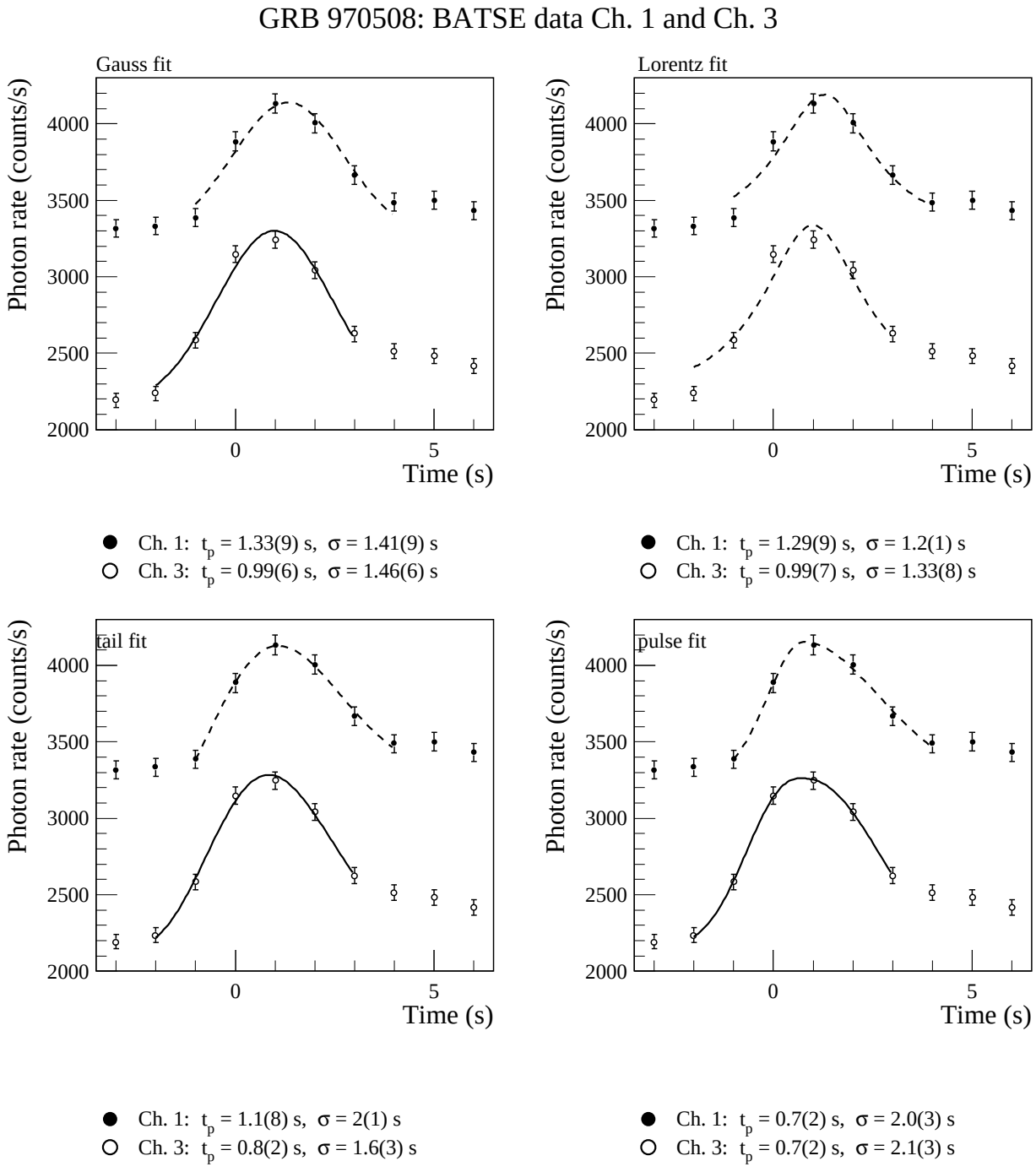


Fig. 1.— *Time distribution of the number of photons observed by BATSE in Channels 1 and 3 for GRB 970508, compared with the following fitting functions: (a) Gaussian, (b) Lorentzian, (c) 'tail' function, and (d) 'pulse' function. We list below each panel the positions $t_p$ and widths $\sigma_p$ (with statistical errors) found for each peak in each fit. We recall that the BATSE data are binned in periods of 1.024 s.*

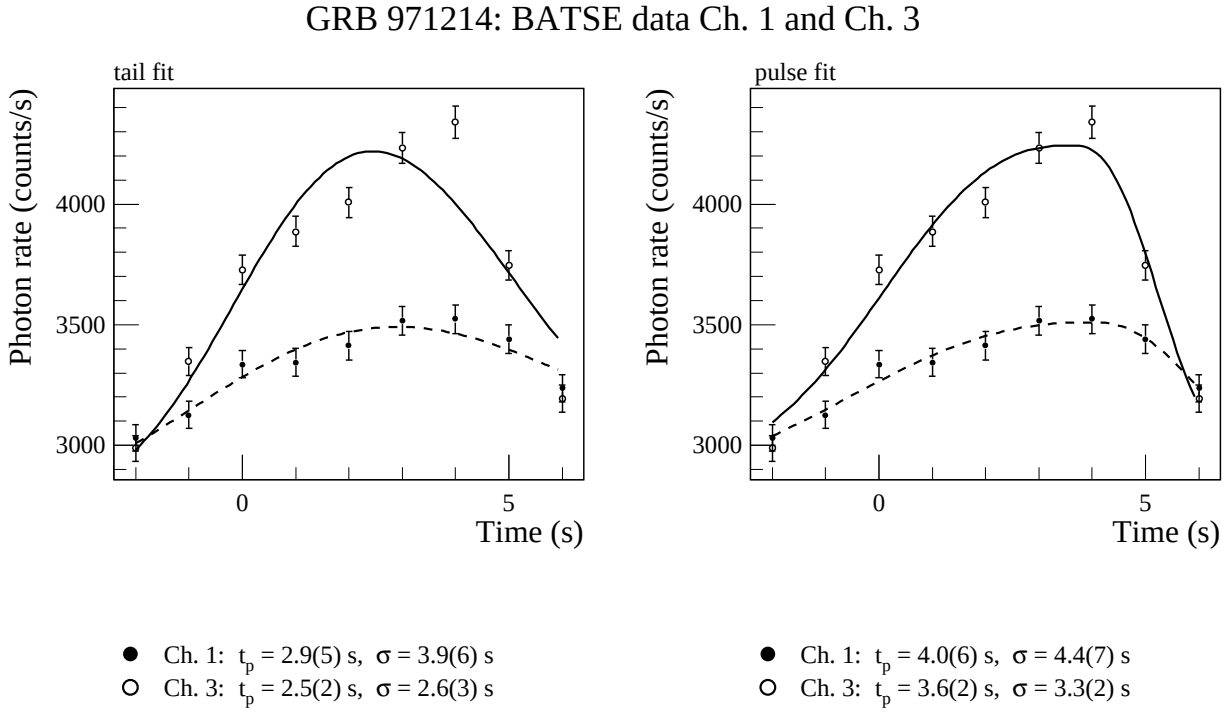


Fig. 2.— *Time distribution of the number of photons observed by BATSE in Channels 1 and 3 for GRB 971214, compared with the following fitting functions: (a) 'tail' function, and (b) 'pulse' function. We list below each panel the positions $t_p$ and widths $\sigma_p$ (with statistical errors) found for each peak in each fit.*

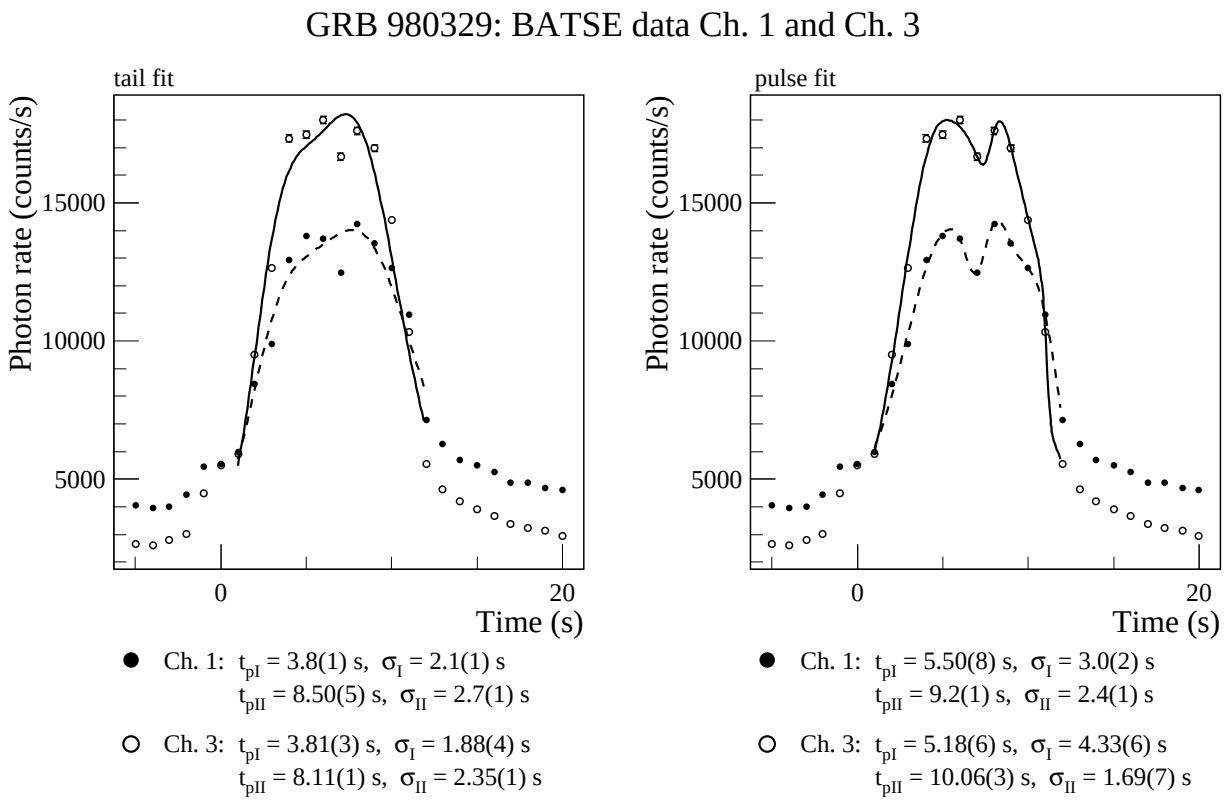


Fig. 3.— *As in fig. 2, but for GRB 980329.*

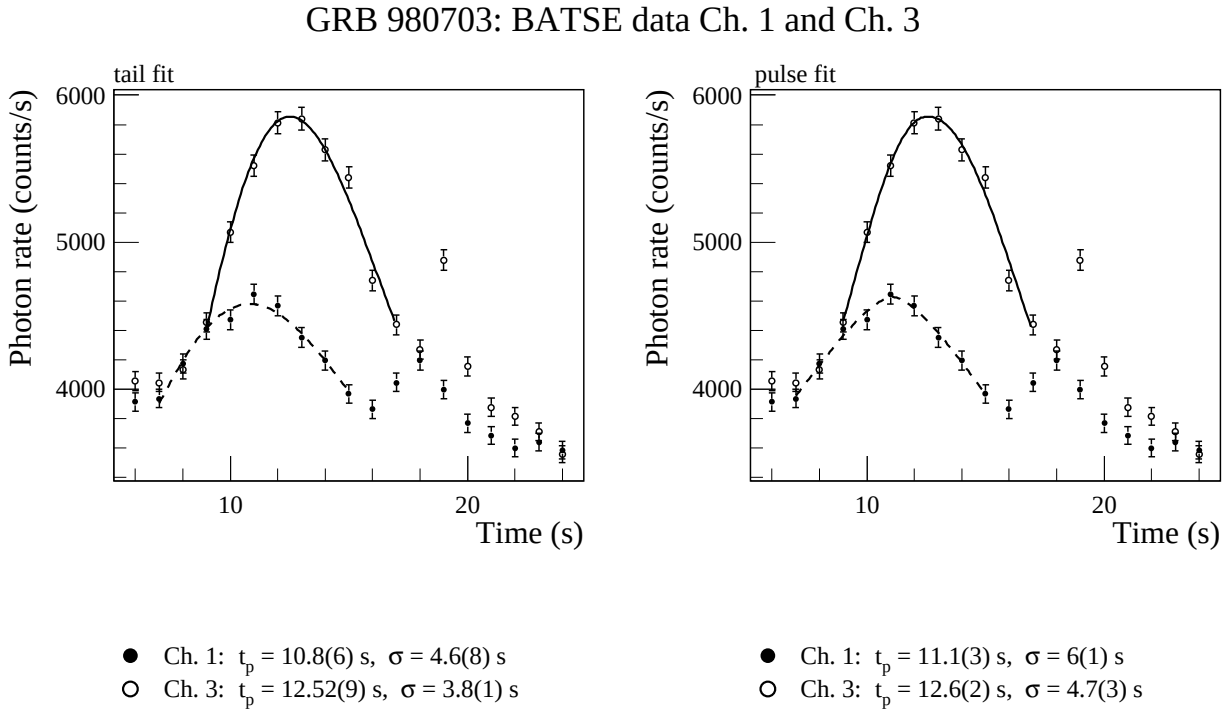


Fig. 4.— *As in fig. 2, but for GRB 980703.*

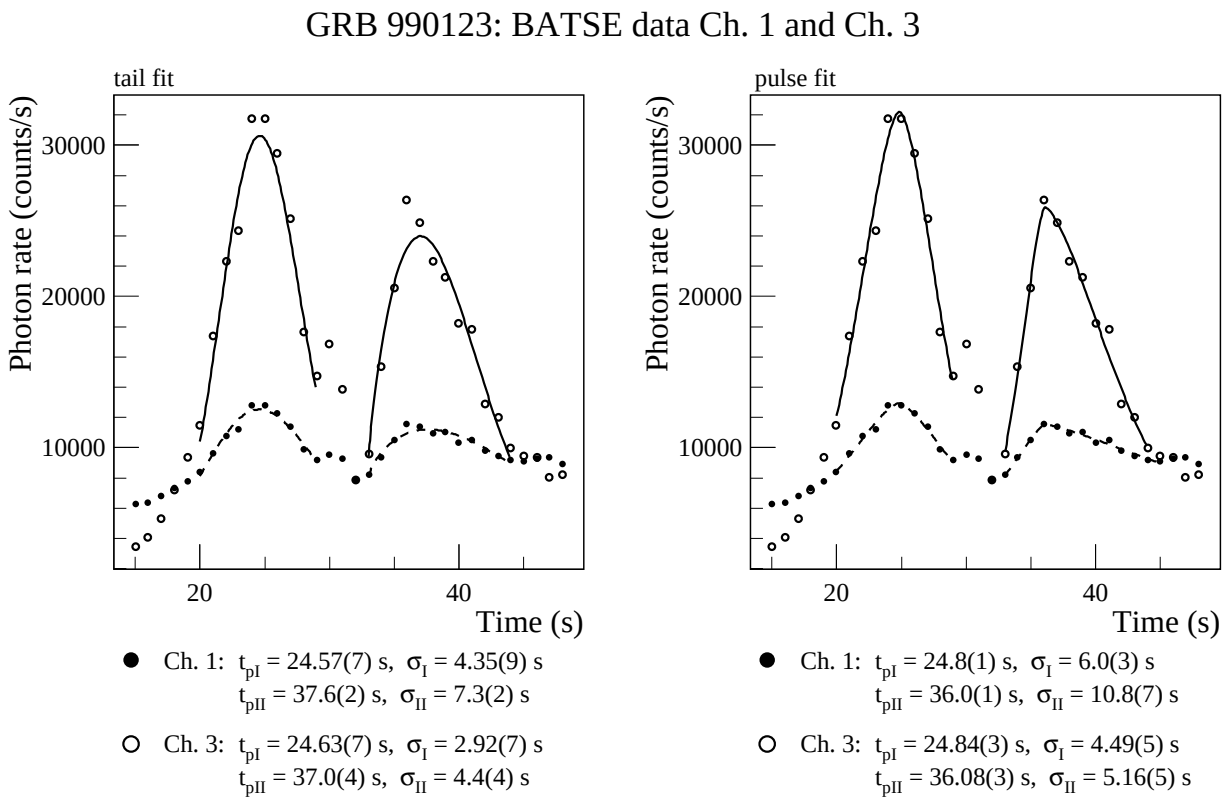


Fig. 5.— *As in fig. 2, but for GRB 990123.*

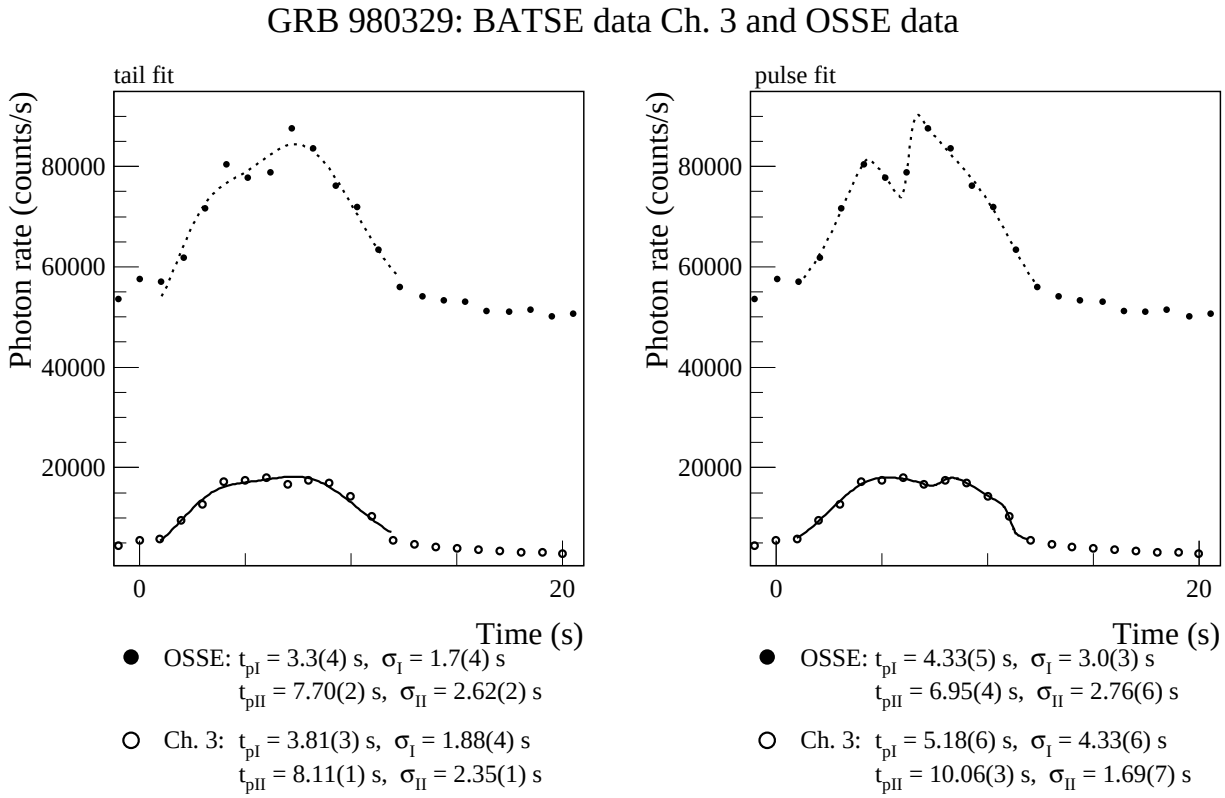


Fig. 6.— *Time distribution of the number of photons observed by OSSE and by BATSE in Channel 3 for GRB 980329, compared with the following fitting functions: (a) 'tail' function, and (b) 'pulse' function. We list below each panel the positions $t_p$ and widths $\sigma_p$ (with statistical errors) found for each peak in each fit.*

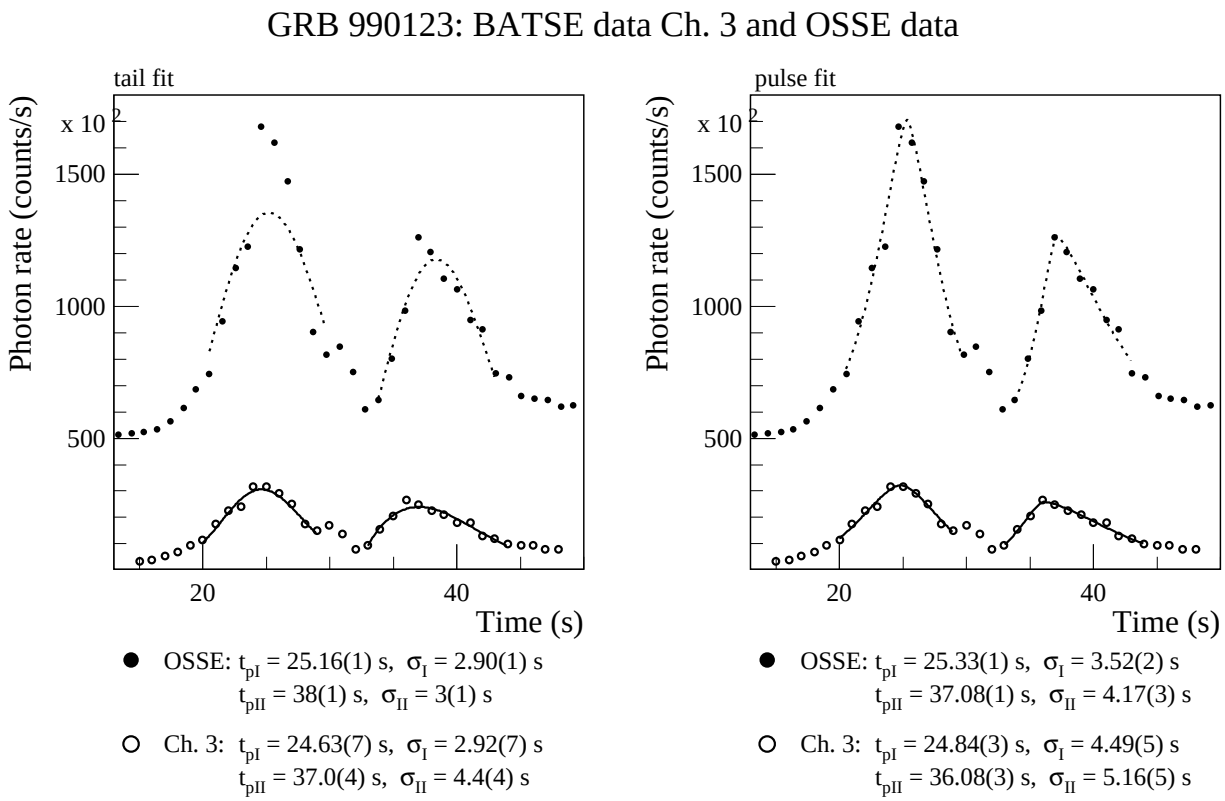


Fig. 7.— *As in Fig. 6, but for GRB 990123.*

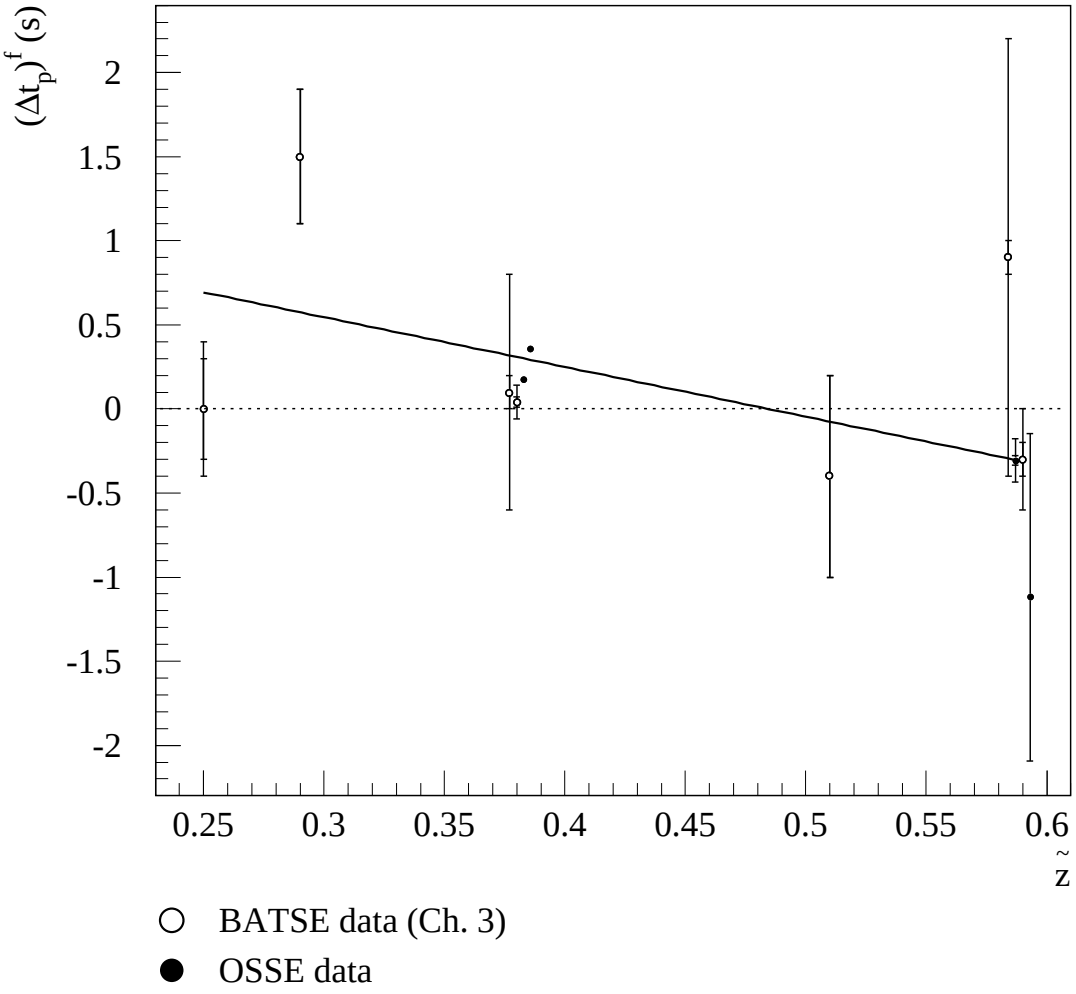


Fig. 8.— *Values of the shifts $(\Delta t_p)^f$ in the timings of the peaks fitted for each GRB studied using BATSE and OSSE data, plotted versus $\tilde{z} = 1 - (1+z)^{-1/2}$, where $z$ is the redshift. The indicated errors are the statistical errors in the 'pulse' fits provided by the fitting routine, combined with systematic error estimates obtained by comparing the results obtained using the 'tail' fitting function. The values obtained by comparing OSSE with BATSE Channel 3 data have been rescaled by the factor $(E_{min}^{BATSE\ Ch.\ 3} - E_{max}^{BATSE\ Ch.\ 1})/(E_{min}^{OSSE} - E_{max}^{BATSE\ Ch.\ 3})$, so as to make them directly comparable with the comparisons of BATSE Channels 1 and 3. The solid line is the best linear fit.*

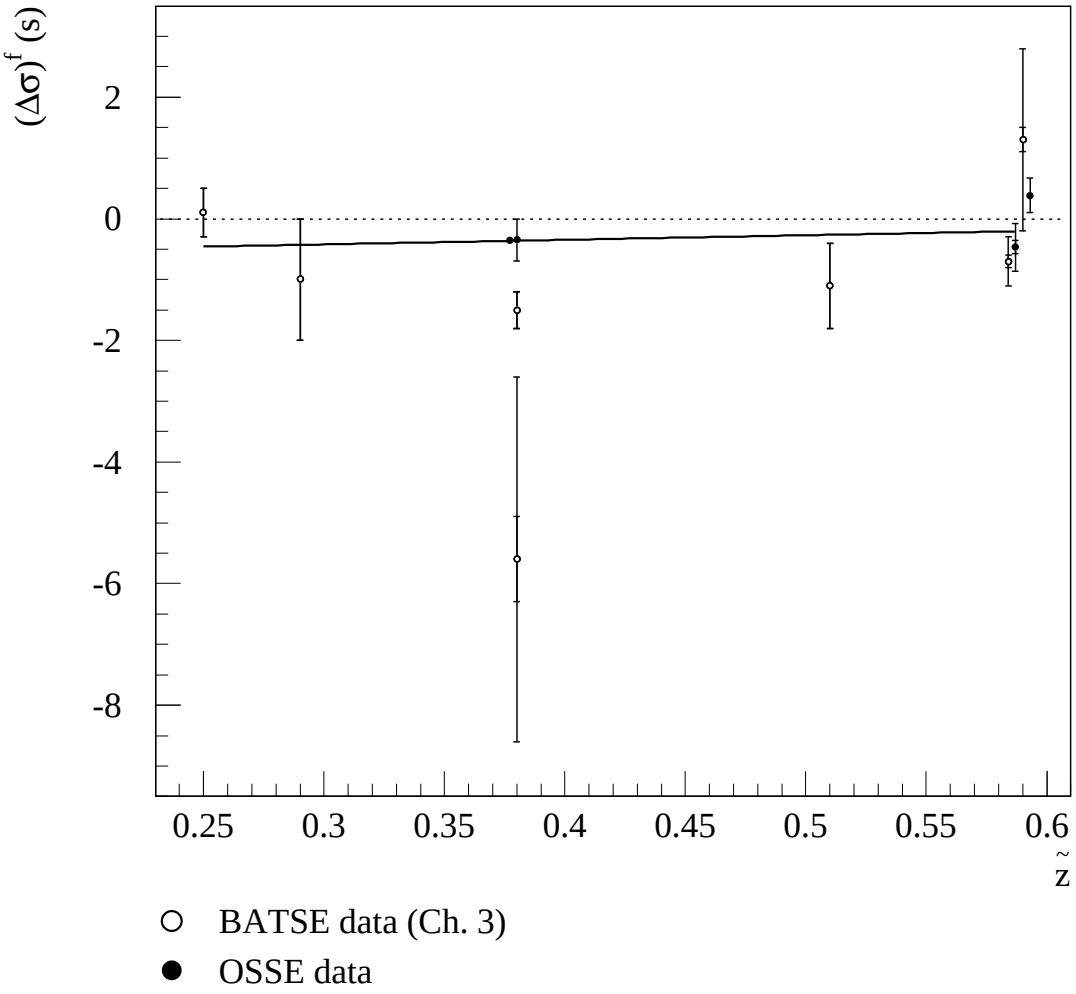


Fig. 9.— *Values of the changes $(\Delta\sigma)^f$ in the widths of the peaks fitted for each GRB studied using BATSE and OSSE data, plotted versus $\tilde{z} = 1 - (1+z)^{-1/2}$, where $z$ is the redshift. The indicated errors are the statistical errors in the 'pulse' fits provided by the fitting routine, combined with systematic error estimates obtained by comparing the results obtained using the 'tail' fitting function. The values obtained by comparing OSSE with BATSE Channel 3 data have been rescaled by the factor $(E_{min}^{BATSE\ Ch.\ 3} - E_{max}^{BATSE\ Ch.\ 1})/(E_{min}^{OSSE} - E_{max}^{BATSE\ Ch.\ 3})$, so as to make them directly comparable with the comparisons of BATSE Channels 1 and 3. The solid line is the best linear fit.*

| | | | GRB 970508 | GRB 971214 | GRB 980329 (I) | GRB 980329 (II) | GRB 980703 | GRB 990123 (I) | GRB 990123 (II) |
|---|---|---|---|---|---|---|---|---|---|
| Ch 1 | Tail | $t_p$ (s) | 1.1(8) | 2.9(5) | 3.8(1) | 8.50(5) | 10.8(6) | 24.57(7) | 37.6(2) |
| | | $\sigma$ (s) | 2(1) | 3.9(6) | 2.1(1) | 2.7(1) | 4.6(8) | 4.35(9) | 7.3(2) |
| | | $t_p$ (s) | 0.7(2) | 4.0(6) | 5.50(8) | 9.2(1) | 11.1(3) | 24.8(1) | 36.0(1) |
| | Pulse | $\sigma_r$ (s) | 1.3(3) | 5.8(3) | 3.65(9) | 1.9(1) | 7(1) | 6.1(2) | 4.6(2) |
| | | $\sigma_d$ (s) | 2.7(3) | 3(1) | 2.3(2) | 2.8(1) | 6(1) | 6.0(3) | 17(1) |
| | | $\sigma$ (s) | 2.0(3) | 4.4(7) | 3.0(2) | 2.4(1) | 6(1) | 6.0(3) | 10.8(7) |
| Ch 3 | Tail | $t_p$ (s) | 0.8(2) | 2.5(2) | 3.81(3) | 8.11(1) | 12.52(9) | 24.63(7) | 37.0(4) |
| | | $\sigma$ (s) | 1.6(3) | 2.6(3) | 1.88(4) | 2.35(1) | 3.8(1) | 2.92(7) | 4.4(4) |
| | | $t_p$ (s) | 0.7(2) | 3.6(2) | 5.18(6) | 10.06(3) | 12.6(2) | 24.84(3) | 36.08(3) |
| | Pulse | $\sigma_r$ (s) | 1.8(3) | 4.6(2) | 3.37(6) | 2.3(1) | 4.3(3) | 4.59(4) | 2.85(4) |
| | | $\sigma_d$ (s) | 2.5(3) | 2.1(2) | 5.28(6) | 1.071(7) | 5.2(3) | 4.39(5) | 7.48(5) |
| | | $\sigma$ (s) | 2.1(3) | 3.3(2) | 4.33(6) | 1.69(7) | 4.7(3) | 4.49(5) | 5.16(5) |
| $\Delta$ | Tail | $\Delta t_p$ (s) | -0.3(8) | -0.4(5) | 0.0(1) | -0.39(5) | 1.7(6) | 0.1(1) | -0.6(4) |
| | | $\Delta\sigma$ (s) | 0(1) | -1.3(7) | -0.2(1) | -0.3(1) | -0.8(8) | -1.4(1) | -2.9(4) |
| | Pulse | $\Delta t_p$ (s) | 0.0(3) | -0.4(6) | -0.3(1) | 0.9(1) | 1.5(4) | 0.04(3) | 0.1(1) |
| | | $\Delta\sigma$ (s) | 0.1(4) | -1.1(7) | 1.3(2) | -0.7(1) | -1(1) | -1.5(3) | -5.6(7) |
| | | $(\Delta t_p)^{\rm f}$ (s) | 0.0(3)(3) | -0.4(6)(0) | -0.3(1)(3) | 0.9(1)(13) | 1.5(4)(2) | 0.04(3)(10) | 0.1(1)(7) |
| | | $(\Delta\sigma)^{\rm f}$ (s) | 0.1(4)(1) | -1.1(7)(2) | 1.3(2)(15) | -0.7(1)(4) | -1(1)(0.2) | -1.5(3)(1) | -5.6(7)(27) |

Table 2: *Results of fits to the GRB data from BATSE. For $A = t_p, \sigma$ in each case, the quantities $\Delta A$ denote the differences $\Delta A \equiv A^{\rm Ch.3} - A^{\rm Ch.1}$, and the quantities $(\Delta A)^{\rm f} \equiv (\Delta A)^{pulse}(\sqrt{\delta A^2_{(1)} + \delta A^2_{(3)}})(\delta(\Delta A))$ are our final results for the induced time delays or width differences of the peaks between BATSE Channels 1 and 3. The first parenthesis in the latter expression denotes the statistical error (where $\delta A_{(i)}$ denotes the statistical error in determining $A$ in the $i^{th}$ channel), whilst the second parenthesis denotes the theoretical "systematic" error, defined as $\delta(\Delta A) \equiv \left|(\Delta A)^{pulse} - (\Delta A)^{tail}\right|$.*

| | | | GRB 980329 (I) | GRB 980329 (II) | GRB 990123 (I) | GRB 990123 (II) |
|---|---|---|---|---|---|---|
| OSSE | Tail | $t_p$ (s) | 3.3(4) | 7.70(2) | 25.16(1) | 38(1) |
| | | $\sigma$ (s) | 1.7(4) | 2.62(2) | 2.90(1) | 3(1) |
| | | $t_p$ (s) | 4.33(5) | 6.95(4) | 25.33(1) | 37.08(1) |
| | Pulse | $\sigma_r$ (s) | 2.39(5) | 0.74(5) | 3.57(2) | 2.26(2) |
| | | $\sigma_d$ (s) | 3.6(4) | 4.78(7) | 3.47(2) | 6.07(4) |
| | | $\sigma$ (s) | 3.0(3) | 2.76(6) | 3.52(2) | 4.17(3) |
| BATSE (Ch. 3) | Tail | $t_p$ (s) | 3.81(3) | 8.11(1) | 24.63(7) | 37.0(4) |
| | | $\sigma$ (s) | 1.88(4) | 2.35(1) | 2.92(7) | 4.4(4) |
| | | $t_p$ (s) | 5.18(6) | 10.06(3) | 24.84(3) | 36.08(3) |
| | Pulse | $\sigma_r$ (s) | 3.37(6) | 2.3(1) | 4.59(4) | 2.85(4) |
| | | $\sigma_d$ (s) | 5.28(6) | 1.071(7) | 4.39(5) | 7.48(5) |
| | | $\sigma$ (s) | 4.33(6) | 1.69(7) | 4.49(5) | 5.16(5) |
| $\Delta$ | Tail | $\Delta t_p$ (s) | -0.5(4) | -0.41(2) | 0.53(7) | 1(1) |
| | | $\Delta\sigma$ (s) | -0.2(4) | 0.27(2) | -0.02(7) | -1(1) |
| | Pulse | $\Delta t_p$ (s) | -0.85(8) | -3.11(5) | 0.49(3) | 1.00(3) |
| | | $\Delta\sigma$ (s) | -1.3(3) | 1.07(9) | -0.97(5) | -0.99(6) |
| | | $(\Delta t_p)^{\rm f}$ (s) | -0.85(8)(35) | -3.11(5)(270) | 0.49(3)(4) | 1.00(3)(0) |
| | | $(\Delta\sigma)^{\rm f}$ (s) | -1.3(3)(11) | 1.07(9)(80) | -0.97(5)(95) | -0.99(6)(1) |

Table 3: *As in Table 2, but comparing fits to data from OSSE, in the range* $1 < E < 5 - 10$ MeV*, and Channel 3 of BATSE.*

## REFERENCES

Ahlen S. *et al.*, AMS Collaboration, 1994, Nucl. Instrum. Meth. A350, 351.

Ashtekar A., 1999, gr–qc/9901023, and references therein.

Amelino-Camelia G., Ellis J., Mavromatos N. E., Nanopoulos D. V. and Sarkar S., 1998, Nature 393, 323;

Amelino-Camelia G., Ellis J., Mavromatos N. E. and Nanopoulos D. V., 1997, Int. J. Mod. Phys. A12, 607.

Biller S. D. *et. al.*, 1998, gr-qc/9810044.

Bloom E. D. *et al.*, GLAST Team, 1996, *Proc. Intern. Heidelberg Workshop on TeV Gamma-Ray Astrophysics*, eds. H.J. Volk and F.A. Aharonian (Kluwer, 1996), 109.

Boella G. *et al.*, BeppoSAX Project, 1997, Astronomy and Astrophysics Supplement Series 122, 327.

Covino S. *et al.*, 1999, astro-ph/9906319.

Ellis J., Hagelin J., Nanopoulos D. V., and Srednicki M., 1984, Nucl. Phys. B241, 381.

Ellis J., Mavromatos N. E., Nanopoulos D. V., 1992, Phys. Lett. B293, 37.

Ellis J., Mavromatos N. E., Nanopoulos D. V., 1998, Int. J. Mod. Phys. A13, 1059.

Ellis J., Mavromatos N. E., Nanopoulos D. V., 1999, gr-qc/9904068, Gen. Rel. Grav. in press; gr-qc/9905048, Gen. Rel. Grav. in press.

Ellis J., Kanti P., Mavromatos N. E., Nanopoulos D. V. & Winstanley E., 1998, Mod. Phys. Lett. A13, 303.

Ford L. H., 1995, Phys. Rev. D51, 1692.

Gambini R. and Pullin J., 1999, Phys. Rev. D59, 124021.

Garay L., 1998, Phys. Rev. D58, 124015.

Hawking S., Page D. N. and Pope C. N., 1980, Nucl. Phys. B170[FS1], 283.

Hawking S., 1982, Comm. Math. Phys. 87, 395.

Hurley K., 1998, astro-ph/9812393.

Kaaret P., 1999, astro-ph/9903464.

Landau L. D. and Lifshitz E. M., 1975, *Classical Theory of Fields* (Pergamon Press, 1975), Vol. 2, page 257.

Lizzi F. and Mavromatos N. E., 1997, Phys. Rev. D55, 7859.

Mavromatos N. E. and Szabo R. J., 1998, hep-th/9808124, Phys. Rev. D59, in press.

Norris J. R. *et al.*, 1996, The Astrophysical Journal 459, 393.

OSSE Collaboration, 1999, `http://www.astro.nwu.edu/astro/osse/bursts/`

Paciesas W. S. *et al.*, 1999, *The fourth BATSE Gamma-Ray-Burst Catalogue* (revised), astro-ph/9903205.

Piran T., 1999, Physics Reports 314, 575.

Rees M., 1997, astro-ph/9701162.

Ricker G., 1998, in *Proc. Conference on Gamma-Ray Bursts in the Afterglow Era*, Rome, November 1998, Astronomy and Astrophysics Supplement Series, to appear;

Scargle J. D., Norris J., and Bonnell J., 1997, astro-ph/9712016.

Schaefer B., 1998, astro-ph/9810479.

Weinberg S., 1972, *Gravitation and Cosmology: Principles and Applications of the General Theory of Relativity* (Wiley, New York, 1972).

Wheeler J. A., 1963, in *Relativity, Groups and Topology*, eds. B.S. and C.M. de Witt (Gordon and Breach, New York, 1963).

Wijers R. A. M. J. *et al.*, 1999, astro-ph/9906346.

Yu H. and Ford L. H., 1999, gr-qc/9904082.